Article
Advanced Science, Engineering and Medicine
Vol. 9, 1–7, 2017
www.aspbs.com/asem

Synthesis of Graphene Oxide/Polyaniline Composites for Hydrogen Storage

Rajveer Singh Rajaura[1,*], Subodh Srivastav[3,*], Vinay Sharma[1], Preetam K. Sharma[1], Ram Gopal[3], Nihal Singh[3], S. Sharma[4], and Y. K. Vijay[3]

[1]Department of Physics, University of Rajasthan, Jaipur 302004, India
[2]Department of Physics, Vivekananda Global University, Jaipur 303905, India
[3]Department of Chemistry, University of Rajasthan, Jaipur 302004, India
[4]Government Women Engineering College, Ajmer 305002, India

In the present work, we synthesized graphene oxide/polyaniline (GO-PANI) composites using *in situ* chemical oxidative polymerization method and investigate their hydrogen storage properties. The morphological and structural properties of synthesized composites have been studied using scanning electron microscopy (SEM), transmission electron microscopy (TEM), X-ray diffraction (XRD) and Raman Spectroscopy. SEM images showed the uneven granular shaped structure of GO-PANI composite, where polyaniline (PANI) wrapped smoothly on the surface of graphene oxide (GO) flakes. The characteristic peaks appeared in XRD and Raman spectrum clearly revealed the structural phase and chemical identity of the composite. The hydrogen adsorption capacity of PANI, GO-PANI and GO composite was determined at room temperature and observed to be 0.47, 0.80 and 1.90 wt.% respectively. The low storage density for GO-PANI nanocomposite might be due to the PANI matrix which wrapped on the surface of graphene oxide. This results in the reduction of reactive surface area, porosity and interrupts functional group with aniline molecules and reduces the interlayer distance. Whereas, for graphene oxide, functional groups work as spacer in between graphene layers which, in turn, increase the interlayer distance to enhance storage density.

Keywords: Graphene Oxide, *In-Situ* Chemical Synthesis, Polyaniline, Materials' Characterisation, Hydrogen Storage Capacity.

1. INTRODUCTION

Discovering new perspectives for environment friendly energy sources and technologies to replace fossil fuels to meet the ever increasing energy demand is one of the grand challenges of the world.[1] In this context, Hydrogen is a renewable, efficient, environmentally friendly and ideal green fuel energy source and has potential to substitute non-renewable carbon based energy system for household and transport applications.[2,3] Hydrogen is a clean-energy fuel as during combustion it produces only water as its byproducts. At the moment, most of the hydrogen is produced by natural gas reforming. However, novel methods for hydrogen production namely photo catalytic water splitting and solar cell-electrolyser combination are not very far from reality.[4] Apart from production, hydrogen storage is clearly one of the challenges in developing hydrogen market due to its ultra-lightweight. Three issues related with the storage should be considered (a) high storage capacity, (b) storage stability, (c) fast kinetic.[5,6] Hydrogen can be stored as (i) pressurized gas, (ii) cryogenic liquid, (iii) solid fuel as chemical (metal hydrate) or physical combination (carbonmaterial).[7,8] The high pressure hydrogen storage requires leak-tight high pressure storage tanks and high mechanical strength piston pump. Due to the low density of hydrogen and the dangerous high pressures of the cylinders, it is not viable for on-board automobile storage. The cryogenic hydrogen storage requires the low temperature for liquefaction that can consume ~40% of total energy. The high electrical requirement and the inevitable boil-off rate, this method is not suitable found for automobile application.[9] Therefore,

*Authors to whom correspondence should be addressed.

solid state hydrogen storage[8, 10] is most encouraging technique which can divide three processes:
(a) chemical absorption in which to the material forming an atomic bond with the absorbing hydrogen molecules,[11]
(b) Composite polymer/metal materials in which engineering hybrid materials with physisorption and chemisorption of hydrogen[12] and
(c) Physical Adsorption in high surface area Materials in which hydrogen molecules physisorption by weak Van der Waals forces.

Carbon nanostructure is one of the most attractive adsorbent for hydrogen storage because of high mechanical strength, high surface area with highly porous, long life cycle and effective heat transfer. The second important criterion for an efficient storage system is the appropriate thermodynamics, fast kinetics. In addition, carbon materials have advantage of being lighter than other inorganic compounds.[13–18] In 2004 Geim and Novoselov used scotch tape to peel off a new material from graphite named graphene. Graphene is two dimensional single layer of sp^2 bonded carbon, has many exciting and wonder properties exploitable for hydrogen storage.[19] The hydrogen storage in graphene has been reported about to be 1.2 wt.% and 0.1 wt.% under a low pressure and different temperature.[20] However, Liu et al.[21] showed the hydrogen storage capacity of MWCNTs and GO 0.9 wt.% and 1.2 wt.% respectively at room temperature. On the other hand, conducting polymers also have been extensively studied and widely applied in various application.[22] PANI is conducting polymers with good eco-friendly nature, high stability, interesting electro activity and unusual doping/dedoping chemistry. PANI can be synthesized through various chemical synthesis methods and widely used for the engineering biosensors, actuators, memory device, chemical sensors, batteries and super capacitors.[23–25] Stefano's et al. investigated a hydrogen storage property of PANI with multi wall carbon nanotube, tine oxide and aluminum powder at temperate range of 298–398 K and pressure 6–7 MPa. The hydrogen storage capacity of pristine PANI has been reported ≈0.35 wt.% which has been enhanced up to 0.5 wt% for PANI-aluminum nano composite.[26] Geckeler et al. reported that HCl doped Polyaniline nano fiber show a hydrogen storage capacity ≈0.46 wt%, whereas Polyaniline-polypyrrole composite can store 0.91 wt% of hydrogen at room temperature and 8 MPa.[27]

In the field of hydrogen energy research, many researchers are focusing to synthesize the different type of graphene based derivatives and modified them with conducting polymers to make a suitable material for enhance hydrogen storage. This further increased the porous structure of the nanocomposites and opening the numbers of binding sites, which in turn enhances the hydrogen storage capacity. In this concern, we have synthesized GO-PANI composite by *in-situ* chemical oxidative polymerization method and used it for hydrogen storage application. Surface morphology and chemical structure of the material is characterized by SEM, TEM, XRD and Raman Spectroscopy. In addition, we have found low storage density of Go-PANI which may be due to that PANI wrapped on the surface of graphene oxide nano sheet that reduce the active surface area and interlayer distance between the graphene layers.

2. SYNTHESIS OF NANOMATERIAL

In this paper, the synthesis process is achieved in three steps:
(1) synthesis of PANI nanoparticle by *in-situ* oxidative polymerization
(2) Synthesis of GO by chemical oxidation of graphite powder
(3) Synthesis of GO-PANI composite by *in-situ* polymerization.

2.1. Synthesis of PANI Nanoparticle

PANI nanoparticle synthesized ~~by~~ using chemical oxidative polymerization method.[28] In this chemical reaction, we have used 0.3 M aniline was dissolved in 100 ml of 1 M HCl solution and then cooled in an ice bath. 100 ml of 0.3 M Ammonium persulphate ($(NH_4)_2S_2O_8$) and 1 M HCl solution was added to the aniline solution drop-wise over 2 h with continuous stirring. A bright green color appears. Stirring was continued for 4 hours. Finally, the solution was centrifuged at 7000 rpm for 20 minutes. The supernatant was discarded and the filtrate was washed multiple times with 1 M HCl.

2.2. Synthesis of GO by Chemical Oxidative Treatment

GO was synthesized using a well-known modified Hummer's method.[30] ~~The synthesis of GO~~ have used graphite powder, concentrated sulfuric acid (H_2SO_4), potassium permanganate ($KMnO_4$), sodium nitrate ($NaNO_3$), hydrogen peroxide (H_2O_2) (30%). More details of synthesis of GO has explained in our previous published paper.[29]

2.3. Synthesis of GO-PANI Composite by *In-Situ* Polymerization

The aqueous solution of GO (200 mg/20 mL) was added in 80 ml of 1 M HCL solution and resultant mixture was ultra-sonication 30 min until GO was completely dispersed. 3.5 mL of aniline in 1 M HCl were introduced in aqueous solution of GO. The dispersed solution was ultrasonicated for another 30 min. Then aniline monomer was drop by drop added into the above solution. The resultant mixture was continues stirred for 1 h at 0–5 °C. The 2.23 mg of ammonium per sulfate ($(NH_4)_2S_2O_8$), was dissolve in 25 ml ~~was dissolved in 25 ml~~ aqueous

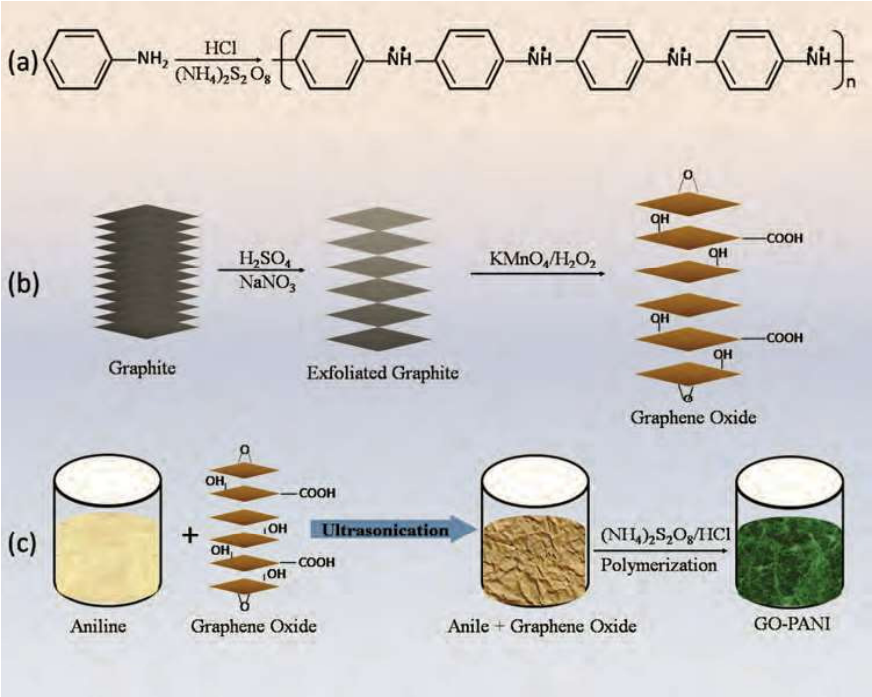

Scheme 1. Overall procedures for synthesis and fabricating of (a) PANI nanoparticle (b) graphene oxide nano sheet, and (c) GO-PANI composite.

HCL solution and the mixture was cooled at 0–5 °C. Further polymerization was achieved by drop wise added of ammonium per sulfate solution in precooled GO solution, and the mixture was stirred for 24 h at 10 °C. The precipitates were collected by filtration and repeatedly washed with deionized water, ethanol, and dried it at 50 °C in vacuum for 24 h.[31]

2.4. Characterization Technique

2.4.1. Characterization

FEI Techni G20-twin TEM microscope at an accelerating voltage of 200 kV was used for morphological characterization. A SEM equipment (Carl Zeiss evo-18) with operating voltage of 20 kV was used and the samples was coated with gold. Structural analysis was carried out using BrukerD8 discover X-ray diffractometer with CuK_{α} X-ray source. Raman measurement was done on an *in-situ* micro Raman (Renishaw, UK) spectroscope with excitation laser beam wavelength of 514.5 nm.

2.4.2. Hydrogen Storage Setup

Hydrogen adsorption was measured ~~by~~ homemade ~~fabricated~~ volumetric apparatus ~~working under~~ 80 bar pressure regions. The configuration, elemental units, detailed design, various tests and operation of the built instrument are similar to those reported by Yang et al.[32] Before measurement storage system was degassed ~~under~~ rotary vacuum ~~measurement~~ and all measurement has been done at room temperature.

3. RESULTS AND DISCUSSION

3.1. Morphology

To visually study of ~~as synthesized composite,~~ the surface morphologies, topography and configurations of the prepared PANI, GO, GO-PANI, are revealed in Figures 1(a)–(f). The PANI Nanoparticle in Figure 1(a) are showing natural entangled highly dense random shaped granular structure.[33] GO in Figure 1(b) is showing conjugated ribbon like highly wavy constitution morphology was observed. It can be due to that structures noticeable as red circle exhibits higher roughness than features represent in yellow circle as well as red circle area are showing few number of layer as compere to darker region indicated by yellow circle area is higher number of layer with defected and agglomeration region of GO. GO-PANI in Figures 1(c)–(d) are showing that PANI nanoparticle smoothly wrapped on each flake of the carbon nano sheets that is indicate the affecting surface morphology of GO by *in-situ* polymerization. The strong affinity between the negatively charged carboxyl groups, hydroxyl group and the positively charged amine nitrogen groups firmly anchors the PANI nanoparticle on GO surface.[34,35] TEM image in Figures 1(e)–(f) of Graphene oxide sheet shown crumpled type structure covered with trimming like regular

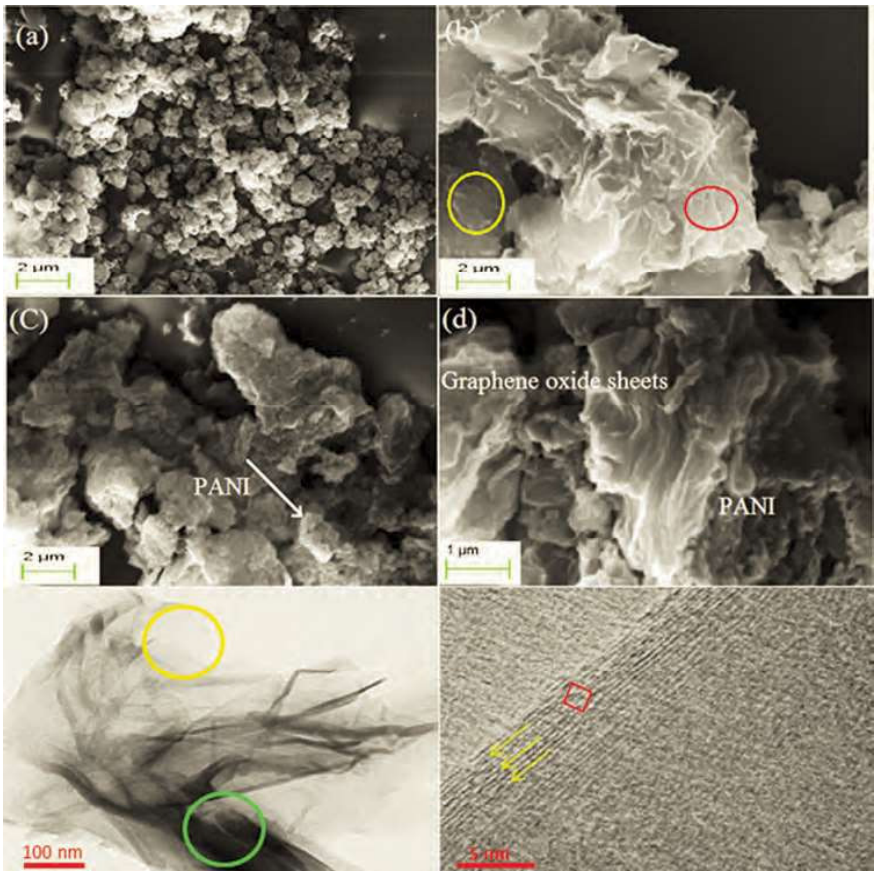

Figure 1. SEM images of (a) PANI nanoparticle (b) as prepared graphene oxide. The difference in color contrast in (b) that is indicated by yellow area circle and read circle area is showing variation of number of graphene layers. (c, d) are showing PANI nano particle is firmly anchor on surface of GO nano sheets. The different image contract of GO in (e) is due to surface topography morphology and density of electron. The dark lines near the edge of graphene oxide in image (f) are indicating the layer thickness and diamond shape is indicating strong deformation lattice of graphene layers.

carbon. Such type of morphology of GO can be ascribed to inter layer bonding between graphene layers due to occurrence of various functional groups that was attached chemical oxidative treatment of graphite powder.[36] Different Image contract of the materials in Figure 1(e) are indicated darker region (green circle area) and lighter region (~~orange~~ circle area) is depend on the surface topography and morphology of as synthesis GO and density of electron. The lighter area is the top surface part of the sample as balance to darker is bottom part of the sample are showing the some defect and impurity in GO nano sheet, which are remaining during solution, purification and draying process. Dark lines near the edges of GO sheet are layer thickness is approximately 8 to 12 nm Figure 1(e), as specified by the yellow arrow line. The diamond shape in Figure 1(f) is marked by using red color in image (f) ~~Shows~~ strong distortion in lattice by ~~using~~ acid treatment and accumulation of graphene layers.[37]

3.2. X-ray Diffraction Analysis

XRD patterns of GO, PANI, GO-PANI Samples shown in Figure 2. The as synthesis GO revel the most intense peak ~~of~~ seeming at 2θ 9.1° ~~with~~ corresponding to interlayer spacing at 8.84 Å.[38] This ~~approach is~~ due treatment of graphite powder with strong acid and oxidizing agent which add the more functional group and water moisture in between interlayer space of GO. This ~~occurrence~~ leads to rise the inter layer space in graphite layer and provide more reactive surface area and increasing the porosity. XRD spectra of PANI nanoparticle show in Figure 2(b) most sharp at 2θ of 14.7°, 20.7°, and 25.3° which corresponding to the (001), (002) and (200) plane.[39] We observed that for GO-PANI composite in Figure 2(c) is showing a weak peak with low intensity and appearing at $2\theta = 11.38$ with agreeing to interlayer distance 7.1 Å, which is lower than GO. The stretched peak of GO-PANI composite is due to disturbance of GO nano sheet with

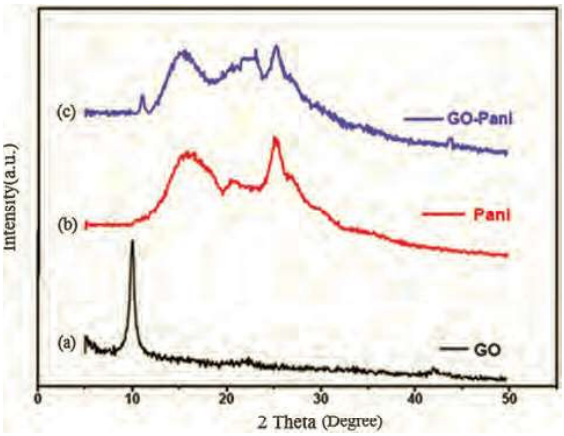

Figure 2. XRD pattern of GO (a) PANI (b) and GO-PANI composite (c).

anchor of PANI nanoparticles and the interaction of functional group of GO with amine nitrogen groups.[40]

3.3. Spectroscopy Analysis

Raman spectroscopy is to further confirm the synthesis of GO and GO-PANI Nano composite, which is powerful technique for the exploring the interaction between PANI and carbon Nano sheet material. ~~In~~ Figure 3 show Raman spectra GO and GO-PANI. The as synthesis GO show the two prominent peak at 1350 to 1605 cm^{-1} are shifted to the 1344 and 1596 cm^{-1} in case of GO-PANI which resemble to well-known D mode, originated by electron phonons coupling or conversion of sp^2-hydridized to sp^3 hybridized and the G mode corresponding to an E_{2g} mode of graphene in-plane vibration of sp^2-bonded carbon atoms, respectively. The intensity of D band is lower than G band in the GO is showing as synthesis GO is high crystal structure of carbon sheet and proposing sheet has low defect and impurity. In the GO-PANI composite intensity

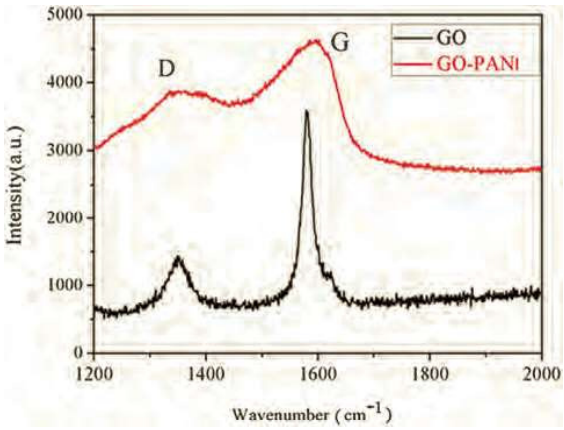

Figure 3. Raman spectral of GO and GO-PANI composite.

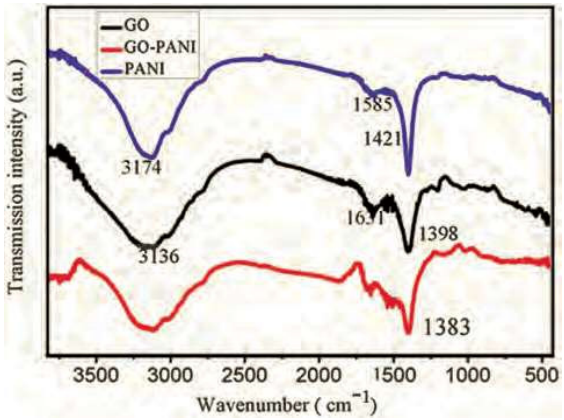

Figure 4. FTIR spectra of GO, PANI, and GO-PANI composite.

of G and D band decrease as well as width of peak also increases, suggesting that sheets have high defect content. Conversely, no clear peak arising from the PANI in composite, due ~~probably to the peak of PANI is weak and or overlapped with the GO peak.~~[41]

The additional evidence in the synthesis of Graphene oxide, PANI, and GO-PANI nanocomposites is provided by the Fourier-transforms infrared spectroscopy (FT-IR) spectra shown in the Figure 4. The typical FT-IR of graphene oxide is showing ~~that~~ peaks located at 3130 cm^{-1}, 1406 cm^{-1}, 1124 cm^{-1}, and 1640 cm^{-1} which shows the O–H and C–O (epoxy or alkoxy), and C═O in carboxylic acid, are present on sample, respectively.[42] The spectrum of PANI in Figure 5(d) shows C═C stretching vibration band at 1586 and 1498 cm^{-1} is attributable to the quinonoid and benzenoid, respectively.[42] In addition, a stretching band assigned to C–N also appears at 1306 cm^{-1}. The FT-IR spectrum of GO-PANI (Fig. (c)) with peaks of hydroxyl and carbonyl groups from GO and strong peaks of functional groups from PANI. Based

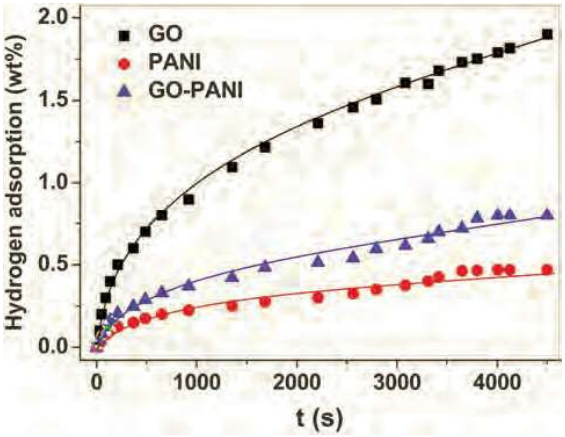

Figure 5. Hydrogen uptakes by GO, PANI and GO-PANI composite.

on FTIR, XFD and morphology of SEM images, it is considered that GO-PANI nanocomposites are effectively synthesized.[43]

4. HYDROGEN STORAGE PERFORMANCE

The hydrogen storages of property of PANI, GO, and GO-PANI have been investigation at room temperature and 80 bar pressure. ~~Outcome of the result, it observed~~ that hydrogen storage of GO (1.90 wt%) is much higher than PANI (0.47 wt%) and GO-PANI (0.80 wt%) shown in the Figure 5.

The Hydrogen storage in PANI are attributing special Electronic structures of PANI and the delocalization of the charge along the polymer backbone chain, which might generate many active sites for interactions with hydrogen. In this regard, Geckeler et al. reported that PANI has outstanding properties such as electronic, thermal, and chemical properties and electrically conducting make it promising materials for hydrogen storage. The thermal treatment of PANI before testing of hydrogen storage at desirable temperature is a very appropriate material for storage because removal of adsorbed water molecules in PANI, thus generating many active sites that is more effective for hydrogen storage.[44,45] However, high storage capacity of hydrogen in GO, is phenomena that a chemical oxidative treatment of graphite powder resultant add the more number of functional group that works as spacer in between the graphite layer and increase the interlayer distance and porosity which leads to add more number of hydrogen molecules on the surface of GO. In this regards, Patchkovskii et al.[46] stated using *ab initio* computations and proposed that H_2 molecules are stored between graphene layers and shown that the interlayer distance plays a key role on the hydrogen storage. They have been perform many experiment to increasing the interlayer distance of graphene layers towards a enhance hydrogen storage capacity. Hydrogen adsorbed graphene in the areas where the local curvature is maximally convex surface but not on concave surface.[47] In the reaction chemistry of synthesis GO, the acid treatment on graphite powder using H_2SO_4 followed by $KMnO_4$ and add on functional on graphene surface can create topological defect that are match with SEM and TEM image in Figure 1 Which might be another region to enrichment of storage density in GO. In this concern, Singh et al. reported using computational simulation the topological defect in on graphene surface play a major role for enriches of hydrogen storage density.[48,49] The low storage density of hydrogen in GO-PANI composite, it seemed that adding the polymer matrix in graphene oxide frame work was reducing the reactive surface area, porosity and interruption of functional group of graphene oxide with aniline molecules and the interaction of GO and PANI is the reduced the interlayer spacing that outcome match with XRD spectra in Figure 2.

5. CONCLUSION

In summary, The GO-PANI composite has been synthesized using *in situ* chemical oxidative polymerization method. The synthesized materials characterized using SEM, TEM, XRD, Raman spectroscopy. A high pressure hydrogen storage Sieverts' setup is indigenously designed, fabricated and installed in our lab for this purpose. Hydrogen storage performance of PANI, GO-PANI and GO at room temperature and high pressure 80 bar was determined by the high pressure volumetric hydrogen storage system. The calculated value of the hydrogen storage capacity for the PANI, GO-PANI and GO are 0.47 0.80 and 1.90 wt.% respectively. The results are explained on the basis of adding the PANI matrix in GO are reducing the reactive surface area, porosity, interruption of functional group with aniline molecules, and reduce the interlayer distance.

Acknowledgments: All author are gratefully acknowledges the financial support by UGC funded project (Reference number-41-903/2012(SR)/UGC), New Delhi, for providing financial assistance.

References and Notes

1. K. Spyrou, D. Gournis, and P. Rudolf, *ECS J. Solid State Sci. Technol.* 2, M3160 (**2010**).
2. E. Tylianakis, G. K. Dimitrakakis, F. J. M. Martinez, S. Melchor, J. A. Dobado, E. Klontzas, and G. E. Froudakis, *Int. J. Hydrogen Energy* 39, 9825 (**2014**).
3. S. Satyapal, J. Petrovic, C. Read, G. Thomas, and G. Ordaz, *Catal. Today* 120, 246 (**2007**).
4. R. W. Bentley, *Energy Policy* 30, 189 (**2002**).
5. A. Züttel, *Mater. Today* 6, 24 (**2003**).
6. I. P. Jain, C. Lal, and A. Jain, *Int. J. Hydrogen Energy* 35, 5133 (**2010**).
7. M. Fichtner, *Adv. Eng. Mater.* 7, 443 (**2005**).
8. L. Schlapbach and A. Züttel, *Nature* 414, 353 (**2001**).
9. L. Zhou, Y. Zhou, and Y. Sun, *Int. J. Hydrogen Energy* 31, 259 (**2006**).
10. B. Sakintuna, F. L. Darkrim, and M. Hirscher, *Int. J. Hydrogen Energy* 32, 1121 (**2007**).
11. R. Bardhan, A. M. Ruminski, A. Brand, and J. J. Urban, *Energy Environ Sci.* 41, 4882 (**2011**).
12. Z. Qr, G. Az, L. Xs, and L. Ws, *Int. J. Hydrogen Energy* 29, 481 (**2004**).
13. C. Liu, Y. Y. Fan, M. Liu, H. T. Cong, H. M. Cheng, and M. S. Dresselhaus, *Science* 286, 1127 (**1999**).
14. Y. Y. Fan, B. Liao, M. Liu, and H. M. Cheng, *Carbon* 37, 1649 (**1999**).
15. A. C. Dillon, K. E. H. Gilbert, P. A. Parilla, J. L. Alleman, and G. L. Hornya, *Nature* 386, 377 (**1997**).
16. E. Singh and H. S. Nalwa, *J. Nanosci. Nanotechnol.* 15, 6237 (**2015**).
17. E. Singh and H. S. Nalwa, *Sci. Adv. Mater.* 7, 1863 (**2015**).
18. H. S. Nalwa (ed.), Handbook of Organic Conductive Molecules and Polymers, 4-Volume Set, Wiley, New York (**1997**).
19. A. K. Geim and K. S. Novoselov, *Nat. Mater.* 6, 183 (**2007**).
20. G. Srinivas, Y. Zhu, R. Piner, N. Skipper, M. Ellerby, and R. Ruoff, *Carbon* 48, 630 (**2010**).
21. S. H. Aboutalebi, S. A. Yamini, I. Nevirkovets, K. Konstantinov, and H. K. Liu, *Adv. Energy Mater.* 2, 1439 (**2012**).
22. Y. Zhao, J. Wu, and J. Huang, *J. Am. Chem. Soc.* 131, 3158 (**2009**).

23. J. Huang, S. Virji, B. H. Weiller, and R. B. Kaner, *Chem. Eur. J.* 10, 1314 **(2004)**.
24. C. Li, H. Bai, and G. Shi, *Chem. Soc. Rev.* 38, 2397 **(2009)**.
25. Y. K. Vijay, P. K. Sharma, S. Srivastava, R. S. Rajaura, V. Sharma, S. S. Sharma, and M. Singh, *AIP Conference Proceedings* **(2014)**, Vol. 1591, p. 658.
26. M. U. Jurczyk, A. Kumar, S. Srinivasan, and E. Stefanakos, *Int. J. Hydrogen Energy* 32, 1010 **(2007)**.
27. N. F. Attia and K. E. Geckeler, *Macromol. Rapid Commun.* 43, 931 **(2013)**.
28. S. Srivastava, S. Kumar, V. N. Singh, M. Singh, and Y. K. Vijay, *Int. J. Hydrogen Energy* 36, 6343 **(2010)**.
29. R. S. Rajaura, S. Srivastava, V. Sharma, P. K. Sharma, C. Lal, M. Singh, H. S. Palsania, and Y. K. Vijay, *Int. J. Hydrogen Energy* 41, 9454 **(2016)**.
30. D. C. Marcano, D. V. Kosynkin, J. M. Berlin, A. Sinitskii, Z. Sun, A. Slesarev, L. B. Alemany, W. Lu, and J. M. Tour, *ACS Nano* 4, 4806 **(2010)**.
31. W. L. Zhang, B. J. Park, and H. J. Choi, *Chem. Commun.* 46, 5596 **(2010)**.
32. L. Aj, Jr., T. R. D. Raimondo, and Y. Rt, *Rev. Sci. Instrum.* 79, 063906 **(2008)**.
33. J. Xu, K. Wang, S. Z. Zu, B. H. Han, and Z. Wei, *ACS Nano* 4, 5019 **(2010)**.
34. M. H. Gass, U. Bangert, A. L. Bleloch, P. Wang, R. R. Nair, and A. K. Geim, *Nat. Nanotechnol.* 3, 676 **(2008)**.
35. J. C. Meyer, C. O. Girit, M. F. Crommie, and A. Zettl, *Nature* 454, 319 **(2008)**.
36. J. C. Meyer, C. Kisielowski, R. Erni, M. D. Rossell, M. F. Crommie, and A. Zettl, *Nano Lett.* 8, 3582 **(2008)**.
37. K. Dave, K. H. Park, and M. Dhayal, *RSC Adv.* 5, 95657 **(2015)**.
38. S. Srivastava, S. S. Sharma, S. Agrawal, S. Kumar, M. Singh, and Y. K. Vijay, *Synth. Met.* 160, 529 **(2010)**.
39. D. Gui, Ch. Liu, F. Chen, and J. Liu, *Appl. Surf. Sci.* 307, 172 **(2014)**.
40. A. C. Ferrari, J. C. Meyer, V. Scardaci, C. Casiraghi, M. Lazzeri, F. Mauri, S. Piscanec, D. Jiang, K. S. Novoselov, S. Roth, and A. K. Geim, *Phys. Rev. Lett.* 97, 187401 **(2006)**.
41. Y. Liu, A. R. Deng, A. Z. Wang, and H. Liu, *J. Mater. Chem.* 22, 13619 **(2012)**.
42. A. B. Bourlinos, D. Gournis, D. Petridis, T. Szabo, A. Szeri, and I. Dekany, *Langmuir* 19, 6050 **(2003)**.
43. J. Xu, K. Wang, S.-Z. Zu, B.-H. Han, and Z. Wei, *ACS Nano* 4, 5019 **(2010)**.
44. N. F. Attia and K. E. Geckeler, *Macromol. Rapid Commun.* 34, 1043 **(2013)**.
45. A. G. M. Diarmid, *Presentation at the Department of Energy*, USA, May **(2005)**, http://www.hydrogen.energy.gov/pdfs/Review05/stp_42_macdiarmid.pdf.
46. S. Patchkovskii, J. S. Tse, S. N. Yurchenko, L. Zhechkov, T. Heine, and G. Seifert, *Proc. Natl. Acad. Sci.* 102, 10439 **(2005)**.
47. S. Goler, C. Coletti, V. Tozzini, V. Piazza, T. Mashoff, F. Beltram, V. Pellegrini, and S. Heun, *J. Phys. Chem.* 117, 11506 **(2013)**.
48. S. Yadav, Z. Zhu, and C. V. Singh, *Int. J. Hydrogen Energy* 39, 4981 **(2014)**.
49. P. K. Sharma, V. Sharma, R. S. Rajaura, S. Srivastava, and Y. K. Vijay, *AIP Conference Publishing* **(2016)**, Vol. 1728, p. 020531.

Received: 13 February 2017. Accepted: 17 April 2017.